THE JOURNAL OF BIOLOGICAL CHEMISTRY
Vol. 258, No. 10, Issue of May 25, pp. 6258-6265, 1983
Printed in U.S.A.

Association between Human Erythrocyte Calmodulin and the Cytoplasmic Surface of Human Erythrocyte Membranes*

(Received for publication, August 21, 1982)

Peter Agre‡, Kevin Gardner, and Vann Bennett§

From the Department of Cell Biology and Anatomy, The Johns Hopkins University School of Medicine, Baltimore, Maryland 21205

This report describes Ca^{2+}-dependent binding of ^{125}I-labeled calmodulin (^{125}I-CaM) to erythrocyte membranes and identification of two new CaM-binding proteins. Erythrocyte CaM labeled with ^{125}I-Bolton Hunter reagent fully activated erythrocyte (Ca^{2+} + Mg^{2+})-ATPase. ^{125}I-CaM bound to CaM depleted membranes in a Ca^{2+}-dependent manner with a K_a of 6×10^{-8} M Ca^{2+} and maximum binding at 4×10^{-7} M Ca^{2+}. Only the cytoplasmic surface of the membrane bound ^{125}I-CaM. Binding was inhibited by unlabeled CaM and by trifluoperazine. Reduction of the free Ca^{2+} concentration or addition of trifluoperazine caused a slow reversal of binding. Nanomolar ^{125}I-CaM required several hours to reach binding equilibrium, but the rate was much faster at higher concentrations. Scatchard plots of binding were curvilinear, and a class of high affinity sites was identified with a K_D of 0.5 nM and estimated capacity of 400 sites per cell equivalent for inside-out vesicles (IOVs). The high affinity sites of IOVs most likely correspond to Ca^{2+} transporter since: (*a*) K_a of activation of (Ca^{2+} + Mg^{2+})-ATPase and K_D for binding were nearly identical, and (*b*) partial digestion of IOVs with α-chymotrypsin produced activation of the (Ca^{2+} + Mg^{2+})-ATPase with loss of the high affinity sites. ^{125}I-CaM bound in solution to a class of binding proteins (K_D ~ 55 nM, 7.3 pmol per mg of ghost protein) which were extracted from ghosts by low ionic strength incubation. Soluble binding proteins were covalently cross-linked to ^{125}I-CaM with Lomant's reagent, and 2 bands of 8,000 and 40,000 M_r (M_r of CaM subtracted) and spectrin dimer were observed by sodium dodecyl sulfate-polyacrylamide gel electrophoresis autoradiography. The 8,000 and 40,000 M_r proteins represent a previously unrecognized class of CaM-binding sites which may mediate unexplained Ca^{2+}-induced effects in the erythrocyte.

CaM[1] is a Ca^{2+}-binding protein (M_r = 17,000) which is highly conserved among eukaryotic cells (see monograph in Ref. 1). CaM undergoes a conformational change when complexed with Ca^{2+} permitting it to bind to the regulator domains of certain enzymes (reviewed in Refs. 2-4). Binding of Ca^{2+}-CaM activates CaM-sensitive enzymes in many different cell types including (Ca^{2+} + Mg^{2+})-ATPase in the erythrocyte (5, 6).

Erythrocytes contain micromolar concentrations of CaM (7). Nanomolar CaM fully activates Ca^{2+} transporter (Ca^{2+} + Mg^{2+})-ATPase (8) maintaining cytosolic free Ca^{2+} at $<10^{-6}$ M (9). Elevation of cytosolic free Ca^{2+} produces alterations in erythrocyte filterability and shape (10), but it is uncertain if these changes are governed by CaM-sensitive enzymes. It is also unclear what roles, in addition to activation of (Ca^{2+} + Mg^{2+})-ATPase, the large concentration of CaM plays in the erythrocyte.

Radiolabeled CaM has been used to directly investigate CaM interactions in several systems. Radiolabeled CaM binds to synaptosomal membranes (11) and adipocyte membranes (12), binds to both brain phosphodiesterase (13) and inhibitor protein (14), and binds to proteins in post-synaptic densities (15). Radiolabeled CaM binds to erythrocyte spectrin (16), and the CaM concentration, $\sim 2.5 \times 10^{-6}$ M, is close to both the K_D of the interaction and to the concentration of spectrin. Radiolabeled CaM also binds to proteins related to spectrin in other tissues (17, 18). Erythrocyte (Ca^{2+} + Mg^{2+})-ATPase interacts directly with CaM (19, 20). ^{125}I-CaM binding to erythrocyte membranes revealed a high affinity class of sites with positive cooperativity which was interpreted to represent direct binding to (Ca^{2+} + Mg^{2+})-ATPase (21-23).

This report describes detailed studies of ^{125}I-CaM binding to erythrocyte membranes. The data support the concept that CaM binds to a class of sites on the membrane with high affinity (K_D = 0.5 nM) and that these sites represent (Ca^{2+} + Mg^{2+})-ATPase. In addition two new CaM-binding proteins have been discovered of 8,000 and 40,000 M_r, and these may mediate presently unexplained actions of Ca^{2+} in erythrocytes.

EXPERIMENTAL PROCEDURES

Materials—^{125}I-Bolton Hunter Reagent (2200 Ci/mmol) and a ^{125}I-CaM radioimmunoassay kit were from New England Nuclear. [γ-^{32}P] ATP was from ICN. PMSF, pepstatin A, Hepes, dithiothreitol, Norit A, EGTA, and trifluoperazine were from Sigma. Dithiobis-*N*-hydroxysuccinimidylproprionate (Lomant's reagent) was from Pierce, and gelatin, N.S.P. was from J. T. Baker Chemical Co. Other commercially available reagents were purchased as described (24).

Methods—CaM purification was adapted from a published method (7). Erythrocytes from three units of fresh human blood were washed four times with 150 mM NaCl, passed through a leukocyte filter, and

* This work was supported by National Institutes of Health Grant 1 RO1 AM29808-02 and by a grant from the Muscular Dystrophy Association. The costs of publication of this article were defrayed in part by the payment of page charges. This article must therefore be hereby marked "*advertisement*" in accordance with 18 U.S.C. Section 1734 solely to indicate this fact.

‡ Recipient of Clinical Investigator Award 1 K08 HL00883-01 from the National Institutes of Health. To whom correspondence should be addressed.

§ Recipient of Research Career Development Award 1 KO4 AM00926-01 from the National Institutes of Health.

[1] The abbreviations used are: CaM, calmodulin; ^{125}I-CaM, ^{125}I-labeled calmodulin; PMSF, phenylmethylsulfonyl fluoride; NaEGTA, ethylene glycol bis(β-aminoethyl ether)-*N,N,N′,N′*-tetraacetic acid, sodium salt; Hepes, 4-(2-hydroxyethyl)-1-piperazineethanesulfonic acid; IOVs, spectrin/actin-stripped inside-out vesicles; SDS, sodium dodecyl sulfate; PAGE, polyacrylamide gel electrophoresis.

washed again before lysis in 15 liters of 7.5 mM $NaPO_4$, 1 mM NaEGTA, 10 μg/ml of PMSF, 2 μg/ml of pepstatin A, pH 7.5, 0 °C. Solid NaCl was added to the lysate (to 0.15 M) and 40 ml of DE52 cellulose (cycled in 7.5 mM $NaPO_4$, pH 7.5) was added and stirred for 30 min. The gel was washed white on a sintered glass filter with 0.15 M NaCl in buffer A (7.5 mM $NaPO_4$, 0.1 mM NaEGTA, 0.2 mM dithiothreitol, 1 mM NaN_3, pH 7.5) and then poured into a column and eluted in two steps of buffer A (step 1 with 0.25 M NaCl, step 2 with 0.5 M NaCl). The second eluate was concentrated against polyethylene glycol 6000 flakes, dialyzed against 50 mM NaCl in buffer A, and applied to an AcA 54 Ultrogel column (2.6 × 65 cm) equilibrated with 50 mM NaCl in buffer A. The third A_{280} peak (1.6 × V_0) was dialyzed against 0.15 M NaCl in buffer A and loaded onto a DE52 cellulose column (1 × 14 cm). The column was eluted with a 100-ml linear gradient of 0.15 to 0.6 M NaCl in buffer A. The first peak (eluted at 0.26–0.28 M NaCl) had an absorption spectrum identical with CaM (7) and was >98% pure by SDS-PAGE. This was dialyzed against 50 mM NaCl, 5 mM $NaPO_4$, 1 mM NaN_3, 10 μM $CaCl_2$, pH 7.5, and frozen at −20 °C in aliquots of 0.4 mg of protein/ml. The second peak (0.34–0.5 M NaCl) was probably nucleic acid.

Pure erythrocyte CaM was radiolabeled with ^{125}I-Bolton Hunter reagent (25). One mCi of ^{125}I-reagent (2200 Ci/mmol) in benzene was dried in the original vial with a stream of N_2. Fifty–100 μl of CaM (4–40 μg in 40 mM $NaPO_4$, pH 8.1) were added for 90 min at 0 °C, diluted to 0.5 ml (with 0.5 mg of gelatin in 100 mM Hepes, 1 mM NaN_3, 0.2 mM dithiothreitol and 50 μM $CaCl_2$), and dialyzed overnight at 2 °C against the same buffer. There was 30–55% incorporation of ^{125}I into CaM (determined by 10% trichloroacetic acid precipitation of an aliquot of reaction mixture diluted with bovine albumin carrier), and specific activities ranged from 0.06 to 1.05 mol of ^{125}I per mol of CaM. ^{125}I-CaM was usually diluted to approximately 2 × 10^{-6} cpm/μg by adding unlabeled CaM immediately after the reaction (except when biological activity of ^{125}I-CaM was determined (Fig. 1)). Aliquots were frozen at −20 °C, and binding characteristics were unchanged even after several weeks.

White ghosts were prepared from fresh human blood (24) by lysis in 7.5 mM $NaPO_4$, 1 mM NaEGTA, 10 μg/ml of PMSF, pH 7.5, with a final wash and storage at 0 °C in 10 mM Hepes, 1 mM NaN_3, 0.1 mM dithiothreitol, pH 7.3. IOVs were prepared quantitatively from ghosts as described but omitting the dextran step (26), and IOVs were washed and stored like ghosts. IOV cell equivalents were calculated by comparing the band 3 content of IOVs and ghosts (determined by scanning Coomassie blue stained SDS-PAGE slabs). Fresh ghosts contained ~3.5 × 10^{-10} mg of protein per cell equivalent and IOVs ~2.6 × 10^{-10}. (Ca^{2+} + Mg^{2+})-ATPase was assayed within 24 h and ^{125}I-CaM binding within 3 days.

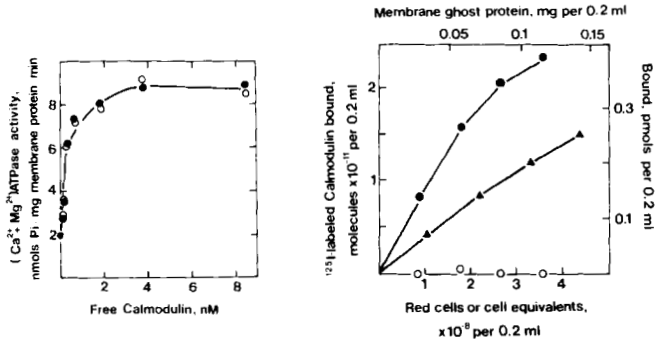

FIG. 1 (*left*). **Effect of increasing concentrations of ^{125}I-CaM (○) and of unlabeled CaM (●) on the activation of erythrocyte membrane-associated (Ca^{2+} + Mg^{2+})-ATPase.** Various concentrations of ^{125}I-CaM (○, 1.05 mol ^{125}I/mol of calmodulin) or unlabeled CaM (●) were incubated with erythrocyte ghosts (16 μg of membrane protein) for 2 h at 0 °C and then 1 h at 24 °C in 0.2 ml of 30 mM KCl, 30 mM Hepes, 80 mM NaCl, 0.5 mM $MgCl_2$, 2.50 mM NaEGTA, 2.486 mM $CaCl_2$ (pCa 5.2), 0.1 mM ouabain, 0.25 mg/ml of gelatin, pH 7.3 (modified from Ref. 44). [γ-^{32}P]ATP (7700 cpm/nmol) (final concentration 0.4 mM) and $MgCl_2$ (final concentration 0.8 mM) were added for an additional hour at 24 °C. Trichloroacetic acid (1.0 ml, 5% w/v, 0 °C) and then Norit A (0.2 ml, 5% w/v) were added and free P_i in the supernatant was determined by counting Cerenkov radiation after centrifugation for 15 min at 4000 × *g*. Basal and CaM-activated (Ca^{2+} + Mg^{2+})-ATPase activity were calculated after subtracting the amount of P_i hydrolyzed in the absence of membranes. Free ^{125}I-CaM concentrations were determined in parallel as described (see under "Methods"). The data are expressed as the average of duplicate determinations.

FIG. 2 (*right*). **Ca^{2+}-dependent binding of ^{125}I-CaM to increasing concentrations of erythrocytes (○), ghosts (●), and IOVs (▲).** Erythrocytes, ghosts, or IOVs were incubated with ^{125}I-CaM (7.2 nM, 44,000 cpm/pmol) for 2 h at 24 °C in 0.2 ml of 0.1 M Hepes, 0.25 mg/ml of gelatin, 2.50 mM NaEGTA, with or without 2.486 mM $CaCl_2$ (pCa^{2+} 5.2), pH 7.3, and Ca^{2+}-dependent membrane-associated counts were determined (see under "Methods").

^{125}I-CaM binding was determined by incubating ^{125}I-CaM (0.25–200 nM) with ghosts or IOVs (10–60 μg of protein). The incubation was in 0.2 ml of 100 mM Hepes containing 0.25 mg/ml of gelatin (a neutral carrier which reduced nonspecific adsorption of subnanomolar CaM concentrations to plastic) and 2.50 mM NaEGTA with or without $CaCl_2$ (providing a specific pCa^{2+} (27)), pH 7.30, in polystyrene tubes (12 × 75 mm) at 24 °C. Bound and free ^{125}I-CaM were separated by layering 0.18 ml over a 0.2-ml sucrose (20% w/v) barrier containing the same buffer with or without $CaCl_2$ in 400-μl hard polyethylene Eppendorf microtest tubes. The tubes were centrifuged for 30 min at 25,000 × *g* and frozen in dry ice. The tips were clipped off and assayed for ^{125}I in a γ counter. Ca^{2+}-independent binding was measured by including 2.50 mM NaEGTA without $CaCl_2$ in the incubation mixtures and sucrose barriers for each concentration of membrane or ^{125}I-CaM, and the value (~0.5% of total cpm added) was subtracted from the corresponding $CaCl_2$-containing sample to yield Ca^{2+}-dependent binding. Values were determined in duplicate and the range was within ±5%.

Resealing of leaky ghosts was checked by centrifugation over 0/10/20% discontinuous Ficoll gradients for 60 min at 100,000 × *g*. Ficoll 400 was dissolved in 100 mM Hepes, 2.50 mM NaEGTA, 2.497 mM $CaCl_2$ (pCa^{2+} 5.0), pH 7.3. Resealed ghosts (prepared in 7.5 mM $NaPO_4$, 1 mM $MgCl_2$, pH 7.5) were impermeable to Ficoll and sedimented to the 0/10% interface while leaky ghosts sedimented to the 10/20% interface. Ghosts incubated with CaM under binding assay conditions did not reseal and still sedimented to the 10/20% interface.

Protein was estimated by the method of Lowry *et al.* (28) using bovine serum albumin as a standard.

RESULTS

Radiolabeled binding proteins must retain biological activity if physiologic conclusions are to be made. CaM radiolabeled with ^{125}I-Bolton Hunter reagent retained full ability to activate brain phosphodiesterase (29), although another report noted such preparations had reduced biological activity (22). The CaM in this report was purified from erythrocytes and radiolabeled with ^{125}I-Bolton Hunter reagent to 1.05 mol of ^{125}I per mol of CaM. ^{125}I-CaM and native CaM activated erythrocyte membrane (Ca^{2+} + Mg^{2+})-ATPase identically (K_a = 0.3 nM, V_{max} = 4.5 × basal, Fig. 1). The erythrocyte ghosts in this study were prepared in buffers containing EGTA and retained less than 0.1% of native erythrocyte CaM (Table I). These ghosts were permeable to large molecules such as Ficoll

TABLE I

Measurement of residual native CaM in CaM-depleted erythrocyte ghosts and IOVs

Erythrocyte ghosts and IOVs were prepared as described under "Methods." After the final wash in 10 mM Hepes, pH 7.3, the following reagents were added making final concentrations: 1 mM dithiothreitol, 1 mM NaEGTA, 1 mM NaN_3, and 2 mM $MgCl_2$. Samples were boiled for 10 min and then centrifuged (100,000 × *g* for 30 min). Supernatants were assayed with a commercial CaM radioimmunoassay kit exactly as directed with controls for buffer effects.

Membranes	CaM Content
	nmol per liter packed cells
Ghosts	2.1
IOVs	1.0[a]
Intact erythrocytes	2500 to 3600[b]

[a] This value is corrected to the volume of the original erythrocytes.
[b] These values are from the literature (16, 23) and were determined by enzyme activation not radioimmunoassay.

and did not reseal during the CaM binding assay (see under "Methods").

Characteristics of Ca^{2+}-dependent ^{125}I-CaM Binding to Erythrocyte Membranes—Ca^{2+}-dependent binding (see below) occurred at intracellular sites and increased linearly with increased concentrations of membranes. Intact erythrocytes failed to bind ^{125}I-CaM (Fig. 2) indicating that binding was restricted to the cytoplasmic membrane surface. Binding to ghosts and IOVs increased linearly up to 0.06 mg of ghost protein per assay, so all studies were conducted in the linear range. IOVs bound less ^{125}I-CaM than ghosts suggesting a loss of binding sites during preparation (see below).

^{125}I-CaM binding depended upon the free Ca^{2+} concentration. Membranes bound negligible ^{125}I-CaM at pCa^{2+} 8.0 but reached maximum at pCa^{2+} 6.4 (Fig. 3). Ca^{2+}-independent binding was subtracted from all data since it was judged to be nonspecific. Ca^{2+}-independent binding did not saturate at increasing concentrations of ^{125}I-CaM (Fig. 8, *A* and *B*), was not reduced by trifluoperazine (Fig. 5), and was not displaced by excess unlabeled CaM (Fig. 4). Furthermore, Ca^{2+}-independent binding was not time dependent.

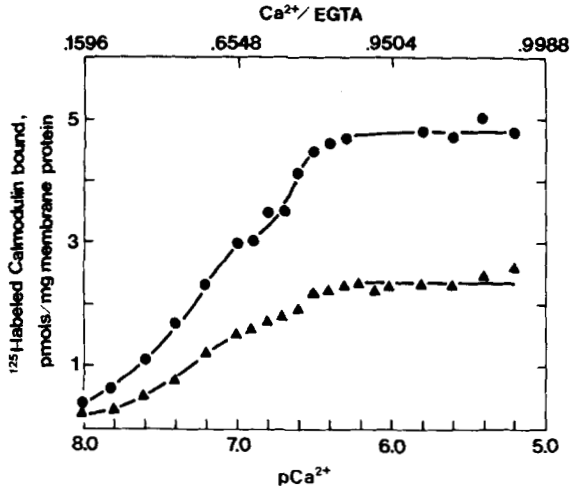

FIG. 3. **Ca^{2+} dependence of ^{125}I-CaM binding to erythrocyte ghosts (●) and IOVs (▲).** Ghosts (0.13 mg of membrane protein/ml) or IOVs (0.12 mg/ml) were incubated with ^{125}I-CaM (30 nM, 27,000 cpm/pmol) in 0.1 M Hepes, 0.25 mg/ml of gelatin, 2.50 mM NaEGTA, pH 7.3, for 2 h at 24 °C. In addition most of the samples contained varying concentrations of $CaCl_2$ (0.399–2.486 mM giving a final pCa^{2+} of 8.0–5.2). Ca^{2+}-dependent binding was determined (see under "Methods").

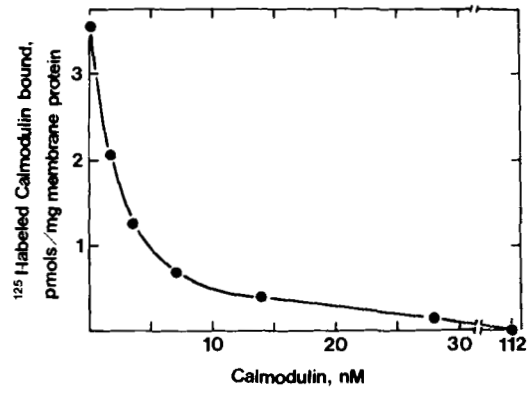

FIG. 4. **Inhibition of Ca^{2+}-dependent binding of ^{125}I-CaM to erythrocyte ghosts by increasing concentrations of unlabeled CaM.** ^{125}I-CaM (1.5 nM, 40,000 cpm/pmol) was incubated for 2 h at 24 °C with ghosts (0.18 mg of membrane protein/ml) in the presence of various concentrations of unlabeled CaM, and Ca^{2+}-dependent binding was determined (see under "Methods").

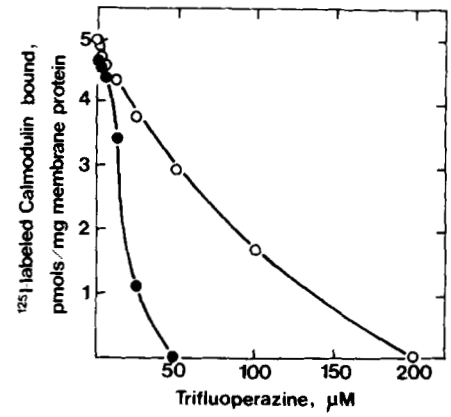

FIG. 5. **Inhibition (●) and reversal (○) of Ca^{2+}-dependent binding of ^{125}I-CaM to erythrocyte ghosts with increasing concentrations of trifluoperazine.** ^{125}I-CaM (12 nM, 45,000 cpm/pmol) was incubated for 90 min at 24 °C with ghosts (0.2 mg of membrane protein/ml) in 0.1 M Hepes, 0.25 mg/ml of gelatin, 2.50 mM NaEGTA, with or without 2.486 mM $CaCl_2$ (pCa^{2+} 5.2), pH 7.3, which also contained various concentrations of trifluoperazine, and inhibition (●) of Ca^{2+}-dependent binding was determined (see under "Methods"). Other samples were incubated identically except that various concentrations of trifluoperazine were added after 60 min and reversal (○) of Ca^{2+}-dependent binding was determined after an additional 60 min of incubation.

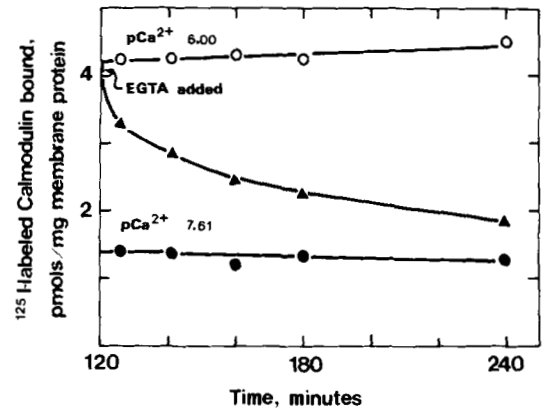

FIG. 6. **Reversal of Ca^{2+}-dependent binding of ^{125}I-CaM to erythrocyte ghosts at various times after reduction of the free Ca^{2+} concentration.** ^{125}I-CaM (14 nM, 45,000 cpm/pmol) was incubated for 2 h at 24 °C with ghosts (0.14 mg of membrane protein/ml) in 0.1 M Hepes, 0.25 mg/ml of gelatin with 2.50 mM NaEGTA, 2.376 mM $CaCl_2$, pH 7.30 (pCa^{2+} 6.00, ○), or with 7.50 mM NaEGTA, 2.376 $CaCl_2$, pH 7.30 (pCa^{2+} 7.61, ●), or with 2.50 mM NaEGTA, 2.376 mM $CaCl_2$, pH 7.30, but with addition of NaEGTA at 120 min to a final concentration of 7.50 mM (pCa^{2+} 6.00 → 7.61, ▲). Aliquots were removed at various times thereafter and Ca^{2+}-dependent binding was determined (see under "Methods").

Ca^{2+}-dependent binding of ^{125}I-CaM was inhibited by both unlabeled CaM and trifluoperazine. Binding of 1.5 nM ^{125}I-CaM was 50% displaced by 2 nM unlabeled CaM and 99% displaced by 112 nM (Fig. 4). Phenothiazines such as trifluoperazine are antagonists of CaM (30). ^{125}I-CaM binding was 50% inhibited by ~15 μM trifluoperazine and at 50 μM caused complete inhibition (Fig. 5).

Membrane-bound ^{125}I-CaM was dissociated by lowering the free Ca^{2+} concentration or by adding trifluoperazine (Figs. 5 and 6). Maximum high affinity binding occurred at pCa^{2+} 6.0. Subsequent addition of EGTA reduced the free Ca^{2+} concentration to pCa^{2+} 7.61, and binding was slowly reversed (Fig. 6). The reversal was biphasic on a semi-log scale with the first

$T_{1/2}$ ~ 18 min and second $T_{1/2}$ ~ 80 min. Dissociation of membrane-bound ^{125}I-CaM required 4-fold greater concentrations of trifluoperazine than required for inhibition of binding. The reversibility is further evidence that the binding is specific and does not represent trapping.

Binding was slow at low concentrations of ^{125}I-CaM (Fig. 7). Binding of 1.5 nM ^{125}I-CaM (a concentration near the K_a for activation of (Ca^{2+} + Mg^{2+})-ATPase) was still increasing slightly after 4 h of incubation. Slow association and slow dissociation indicate that the sites are in slow equilibrium with CaM. The slow off-rate could also influence the extent of extraction of CaM from membranes during ghost preparation (Table I). The on-rate was driven much faster at 60 nM ^{125}I-CaM (Fig. 7). Erythrocytes contain >10^{-6} M CaM (7), so binding may be extremely rapid *in vivo*.

Analysis of Membrane-binding Affinities and Capacities—Binding of ^{125}I-CaM to ghosts and IOVs was measured as a function of CaM concentration (Fig. 8, *A* and *B*). Scatchard plots were curvilinear at equilibrium (Fig. 8*C*) indicating either multiple independent sites or negatively cooperative associations at a single site. Negative cooperativity affecting a single class of sites is unlikely since the high affinity sites were selectively removed by proteolytic digestion (Fig. 10, *inset*), and three different binding proteins have been identified (see below). High affinity binding sites were resolved from lower affinity sites with a reiterative nonlinear two-site fitting program (31). The capacity estimated for ghosts was 4.7 pmol/mg of membrane protein (~1000 high affinity sites per cell) and for IOVs 2.4 pmol/mg (~400 high affinity sites per cell equivalent) assuming K_D = 0.3 nM. These values are ~30% smaller than estimates made by linear extrapolation from the high affinity slope in Fig. 8*C* (ghosts, 6.4 pmol/mg and IOVs, 3.4 pmol/mg). High affinity binding was measured in more detail with several concentrations of ^{125}I-CaM below 1 nM to determine the K_D more accurately (Fig. 9*B*). Double reciprocal binding plots for both ghosts and IOVs indicated that the high affinity binding K_D = 0.5 nM, and this value is essentially identical with the K_a = 0.3 nM for CaM activation of (Ca^{2+} + Mg^{2+})-ATPase measured under identical conditions (Fig. 9*A*).

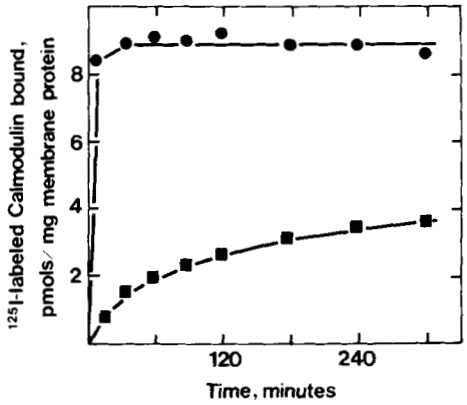

FIG. 7. **Time course of Ca^{2+}-dependent binding of ^{125}I-CaM to erythrocyte ghosts.** ^{125}I-CaM (1.5 nM (■) or 60 nM (●), 44,000 cpm/pmol) was incubated at 24 °C with ghosts (0.17 mg of membrane protein/ml), and Ca^{2+}-dependent binding was measured at various times (see under "Methods").

The IOVs contained only half as many CaM-binding sites and half as much (Ca^{2+} + Mg^{2+})-ATPase activity as ghosts (Figs. 8 and 9). Possible explanations include removal, sequestration, or damage of CaM-binding sites and (Ca^{2+} + Mg^{2+})-ATPase during the low ionic strength extraction procedure. Soluble binding sites were identified in the low ionic strength extract (Fig. 11, see below). It is technically difficult to quantitatively correlate binding of ^{125}I-CaM to membrane sites with binding to soluble sites, and it is likely that the soluble binding estimates are too low. The soluble extract, however, contained very little (Ca^{2+} + Mg^{2+})-ATPase activity (data not shown). It is unlikely that CaM binding sites are sequestered in right-side-out vesicles since the methods used here remove >95% of all spectrin from ghosts yielding >85% inside-out vesicles (26). The reduction in CaM binding sites is probably not due to damage of sites since neither repeated freezing and thawing nor prolonged storage at 0 °C reduced binding (data not shown). (Ca^{2+} + Mg^{2+})-ATPase activity, however, is much more labile with continuous loss of (Ca^{2+} + Mg^{2+})-ATPase activity even when chilled at 0 °C and abrupt loss of activity after exposure to sulfhydryl reactants (data not shown). The Ca^{2+} transporter is an integral membrane protein extractable only with detergents (19) and remains in

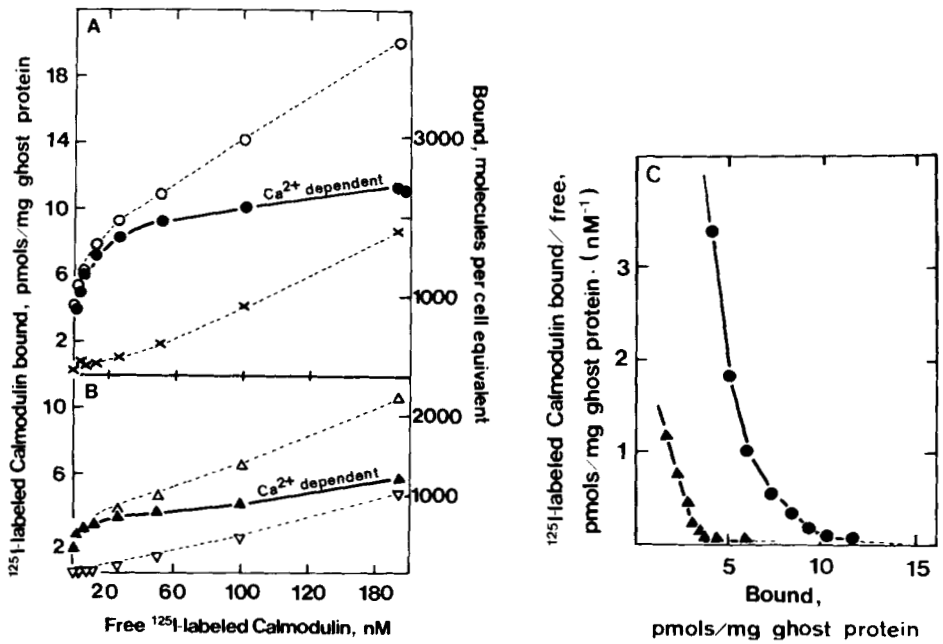

FIG. 8. **Effect of increasing ^{125}I-CaM concentrations on Ca^{2+}-dependent binding to erythrocyte ghosts (●, *A*) and IOVs (▲, *B*).** Various concentrations of ^{125}I-CaM were incubated for 180 min at 24 °C with ghosts (0.15 mg of membrane protein/ml, *A*) and IOVs (0.28 mg of membrane protein/ml, *B*), and Ca^{2+}-dependent binding was determined (see under "Methods"). Binding in 0.1 M Hepes, 0.25 mg/ml of gelatin, 2.50 mM NaEGTA with 2.486 mM $CaCl_2$ (pCa^{2+} 5.2), pH 7.3, ○- - -○, △- - -△; binding in 0.1 M Hepes, 0.25 mg/ml of gelatin 2.50 mM NaEGTA, pH 7.3, ×- - -×, ▽- - -▽. The difference represents Ca^{2+}-dependent binding, ●——●; ▲——▲, and binding to IOVs was corrected to the original ghost protein concentration. Ca^{2+}-dependent binding is presented in *C* according to the Scatchard equation (54): $B/F = N/K - B/K$ where B = pmol of ^{125}I-CaM bound per mg of membrane protein, F = unbound (nanomolar); K = dissociation constant, and N = capacity (pmol/mg).

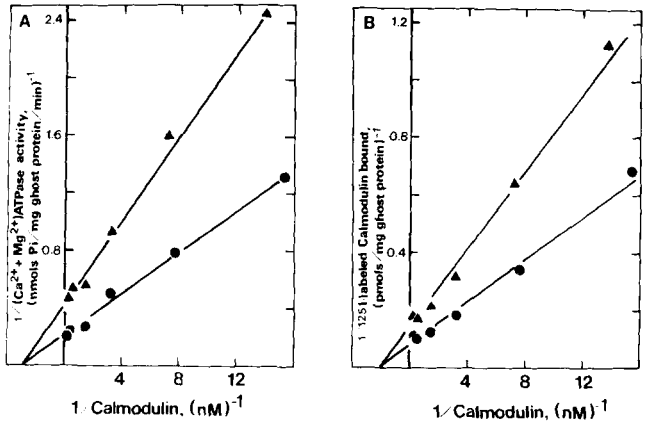

FIG. 9. **Effect of increasing CaM concentrations on (Ca^{2+} + Mg^{2+})-ATPase activity (*A*) and Ca^{2+}-dependent ^{125}I-CaM binding (*B*).** Various concentrations of CaM were incubated for 2 h at 0 °C and then for 1 h at 24 °C with ghosts (●, 0.06 mg of membrane protein/ml) or IOVs (▲, 0.09 mg of membrane protein/ml) in 30 mM KCl, 30 mM Hepes, 80 mM NaCl, 0.5 mM $MgCl_2$, 0.1 mM ouabain, 0.25 mg/ml of gelatin, 2.50 mM NaEGTA, with or without 2.486 mM $CaCl_2$ (pCa 5.2), pH 7.30. In *A* [γ-^{32}P]ATP (1600 cpm/nmol) and $MgCl_2$ were then added (final concentrations of 0.2 mM and 0.4 mM) for an additional hour at 24 °C. (Ca^{2+} + Mg^{2+})-ATPase activity was calculated from the free P_i determinations (see Fig. 1). *B* was identical except that the CaM was ^{125}I-CaM (400,000 cpm/pmol), the ATP was unlabeled, and Ca^{2+}-dependent ^{125}I-CaM binding was determined (see under "Methods"). The K_a for the (Ca^{2+} + Mg^{2+})-ATPase for both ghosts and IOVs is approximately 0.3 mM and the K_D for binding is approximately 0.5 nM.

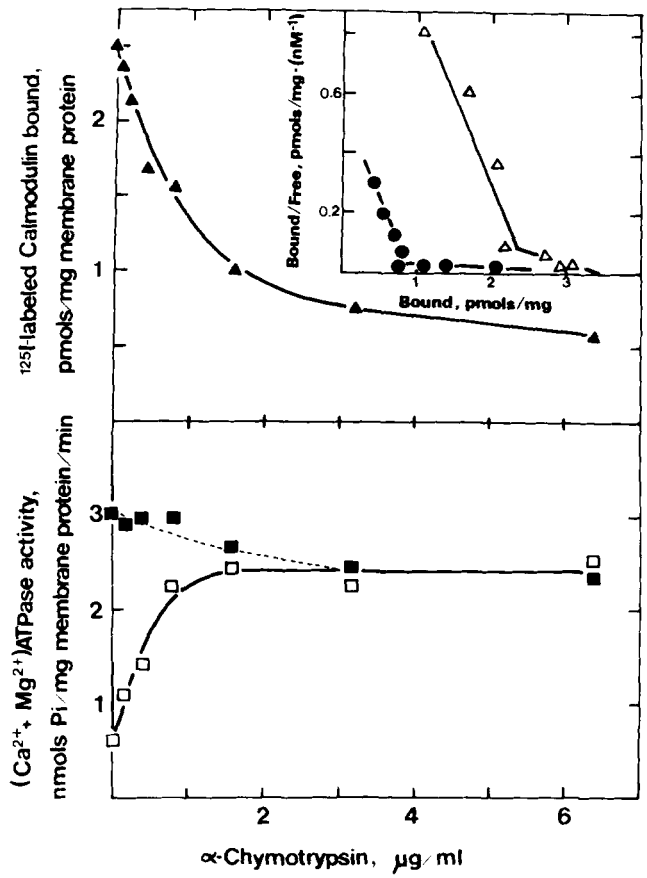

FIG. 10. **Effect of mild α-chymotrypsin digestion of IOVs on Ca^{2+}-dependent binding of ^{125}I-CaM (*top*) and (Ca^{2+} + Mg^{2+})-ATPase (*bottom*).** IOVs were incubated with various concentrations of α-chymotrypsin (0–6.6 μg/ml) in 0.5 ml of 10 mM Hepes, 1 mM NaN_3, 0.5 mM dithiothreitol, pH 7.3, for 45 min at 0 °C. The IOVs were then diluted in 20 volumes of 10 mM Hepes, 50 μg/ml of PMSF and centrifuged (25 min at 44,000 × *g*). The digested IOVs still contained at least 83% of the original protein when resuspended in the original volumes. In the *top panel*, ^{125}I-CaM (14.4 nM, 45,000 cpm/pmol) was incubated for 90 min at 24 °C with the various vesicle pellets (0.1 mg of membrane protein/ml) and Ca^{2+}-dependent ^{125}I-CaM binding was determined (▲) (see under "Methods"). The *inset* contains a Scatchard plot (52) from a similar experiment showing Ca^{2+}-dependent ^{125}I-CaM (1.4–180 nM, 51,000 cpm/pmol) binding to undigested IOVs (△, 0.19 mg of membrane protein/ml) and IOVs digested with 2 μg/ml α-chymotrypsin (●). In the *lower panel* the digested IOVs (0.2 mg of membrane protein/ml) were incubated with [γ-^{32}P]ATP (5,500 cpm/pmol) and $MgCl_2$ (final concentrations 0.125 and 0.3 mM). Basal (no added CaM, □) or stimulated (14 nM CaM, ■) (Ca^{2+} + Mg^{2+})-ATPase activity was calculated from free P_i determinations (see Fig. 1).

the IOV membranes after low ionic strength extraction. These conditions most likely remove a different class of CaM-binding proteins and also remove (or damage) a different class of (Ca^{2+} + Mg^{2+})-ATPase which is inactive in solution.

The high affinity binding sites remaining on IOVs most likely represent binding of ^{125}I-CaM directly to the Ca^{2+} transporter. Estimates of the K_D and K_a were nearly identical (Fig. 9). IOVs were estimated to retain ~400 nonextractable high affinity binding sites per cell equivalent which is the number of (Ca^{2+} + Mg^{2+})-ATPase copies per erythrocyte estimated from studies of phosphorylated intermediates (32). This value is much lower than estimates based on turnover number (33), photoaffinity labeling (34), or direct binding under very different conditions (23). (Ca^{2+} + Mg^{2+})-ATPase was thought to be proteolytically activated by removal of CaM binding sites of the enzyme (20, 35, 36). Mild α-chymotrypsin digestion of IOVs produced activation of the (Ca^{2+} + Mg^{2+})-ATPase with loss of additional CaM stimulation and loss of most high affinity CaM binding sites but sparing of the low affinity sites (Fig. 10). It is unlikely that the ^{125}I-CaM was damaged by persistent traces of α-chymotrypsin since the supernatant (unbound ^{125}I-CaM) subsequently bound well to other membranes (not shown). Interestingly, other CaM-sensitive enzymes are activated in the absence of CaM by partial proteolysis (phosphodiesterase (37), phosphorylase *b* kinase (38), and myosin light chain kinase (39)) suggesting that CaM regulates other enzymes by a similar manner.

Solubilized CaM-binding Sites—It is clear that when IOVs were prepared from ghosts, binding sites were removed (Figs. 2, 3, 8, and 9). Spectrin binds CaM with a $K_D = 2.8 \times 10^{-6}$ M (16), but the binding sites removed during preparation of IOVs were of much higher affinity. These sites were not destroyed since a significant number of sites were recovered in the extract. Binding of ^{125}I-CaM in solution was measured by a modified gel filtration method (Fig. 11 (40)). The *peak* in the *upper panel* represents ^{125}I-CaM excluded from a previously equilibrated column due to Ca^{2+}-dependent interaction with soluble binding sites and was not detected in the absence of Ca^{2+} (*lower panel*). The affinity of the association was estimated by separation of bound and unbound ^{125}I-CaM by gel filtration over a range of ^{125}I-CaM concentrations (Fig. 12). Scatchard plots were curvilinear and tangential extrapolation along each of three regions suggests that different solubilized binding sites exist with most points falling along tangent *Y* (K_D = 55 nM, *N* = 7.3 pmol/mg based upon the original membrane protein). There also appeared to be a very small number of higher affinity sites (slope *X*) and another class of sites (*Z*) which did not approach saturation at 150 nM ^{125}I-labeled CaM.

Solubilized binding sites were identified by covalent cross-linking to ^{125}I-CaM and SDS-PAGE autoradiography (Fig. 13). ^{125}I-CaM has been shown to interact directly with calci-

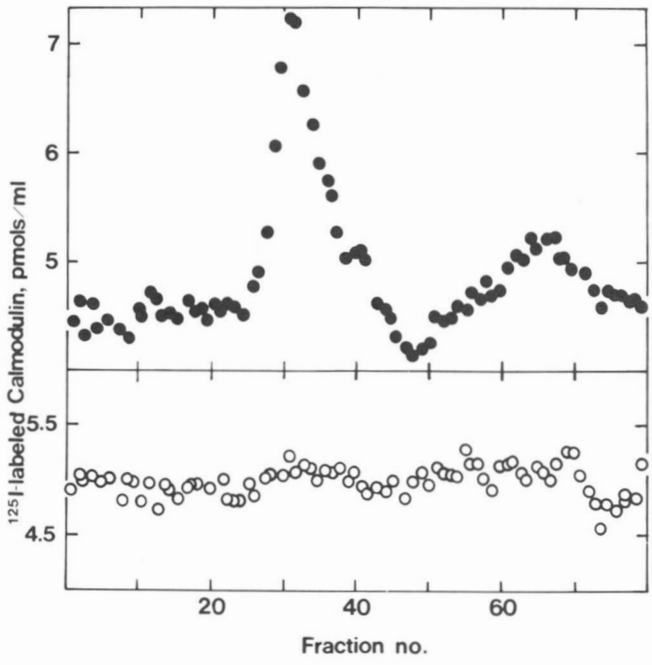

FIG. 11. **Ca^{2+}-dependent binding of ^{125}I-CaM in solution by low ionic strength extract from erythrocyte ghosts.** Binding of ^{125}I-CaM to low ionic strength extract in solution (see under "Methods") was measured using an adaptation of the gel filtration method (40). Extract (0.3 mg of protein/ml) was incubated with ^{125}I-CaM (2.5 nM, 34,000 cpm/pmol) in 0.1 M Hepes, 2.5 mg/ml of gelatin, 0.2 mM dithiothreitol, 2.50 mM NaEGTA, pH 7.3 with (●) or without (○) 2.497 mM $CaCl_2$ (pCa^{2+} 5.0) for 2 h at 4 °C. Volumes of 0.4 ml were loaded into the appropriate number of paired AcA54 Ultragel columns (1 × 25 cm) previously equilibrated with the same buffer (containing ^{125}I-CaM, Hepes, gelatin, dithiothreitol, NaEGTA with or without $CaCl_2$), and the column was eluted at 5 ml/h at 4 °C. Fractions of 0.3 ml were collected and the excluded volume appeared in fraction 30.

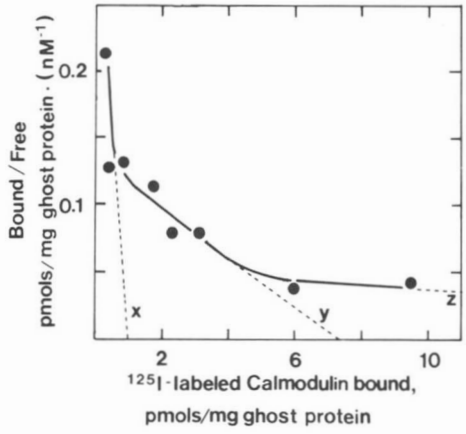

FIG. 12. **Effect of increasing concentrations of ^{125}I-CaM on Ca^{2+}-dependent binding to low ionic extract from erythrocyte ghosts.** Extract (see under "Methods") was incubated with varying amounts of ^{125}I-CaM (2.5–150 nM, 170,000 cpm/pmol) in 0.1 M Hepes, 2.5 mg/ml of gelatin, 0.2 mM dithiothreitol, 2.50 mM NaEGTA, 2.497 mM $CaCl_2$ (pCa^{2+} 5.0) for 2 h at 24 °C. Volumes of 0.1 ml were loaded onto AcA54 Ultragel columns (0.5 × 6 cm) previously equilibrated with the same buffer (without ^{125}I-CaM) and the column was eluted at 9 ml/h at 24 °C while collecting 0.15-ml fractions. The excluded volume (cpm = bound) appeared at 1.3 ml and the retained (cpm = free) appeared at 2.1 ml. *Points* represent duplicate determinations plotted according to the Scatchard equation (54), and three parameters were estimated by linear extrapolations (*x*, *y*, and *z*). Protein concentration refers to mg of protein of the original ghosts from which the extract was made.

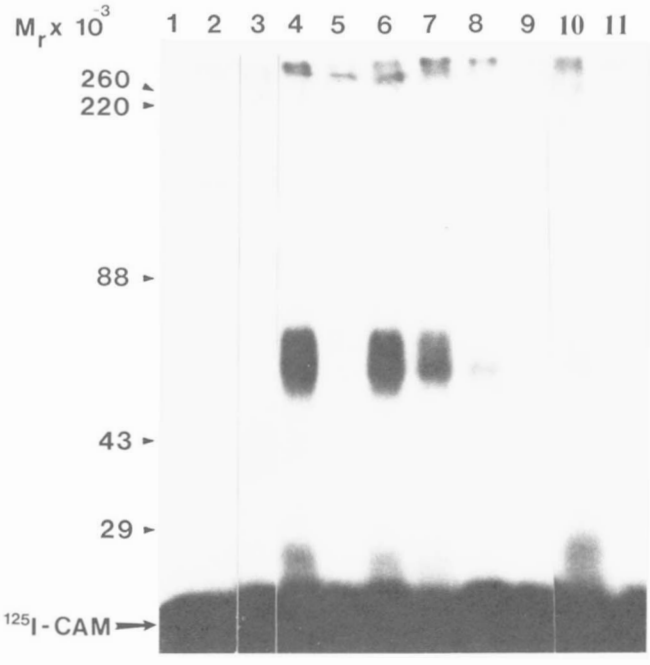

FIG. 13. **Cross-linking of ^{125}I-CaM to low ionic strength extract of erythrocyte ghosts.** Ghosts were extracted in low ionic strength buffer (see under "Methods"), and supernatant ("extract", 0.3 mg of protein/ml) or IOVs (1 mg/ml) were incubated with ^{125}I-CaM (6 nM, 136,000 cpm/pmol) in 0.1 M Hepes, 2.50 mM NaEGTA in the presence or absence of 2.497 mM $CaCl_2$ (pCa^{2+} 5.0) for 2 h at 24 °C under various conditions (in the presence of excess unlabeled CaM or trifluoperazine). Dithiobis-*N*-hydroxysuccinimidylproprionate (a cross-linker, 41) was added (to 0.25 mg/ml) and incubated an additional hour at 4 °C before addition of glycine (to 0.6 mM) to quench the cross-linking. Aliquots were analyzed by SDS-PAGE (Laemmli (55)) adapted to include a 7.5–15% acrylamide gradient with autoradiography. Molecular weight standards were determined by a semilog plot of migration distance of erythrocyte ghosts proteins from a corresponding lane which was stained with Coomassie brilliant blue. All lanes contained ^{125}I-CaM and NaEGTA. In addition: *lane 1*, no cross-linker and no $CaCl_2$; *lane 2*, no cross-linker with $CaCl_2$; *lane 3*, cross-linker and $CaCl_2$ with 12 nM (instead of 6 nM) ^{125}I-CaM; *lane 4*, extract, cross-linker, and $CaCl_2$; *lane 5*, extract and cross-linker without $CaCl_2$; *lane 6*, 20 nM unlabeled CaM, extract, cross-linker, and $CaCl_2$; *lane 7*, 100 nM unlabeled CaM, extract, cross-linker, and $CaCl_2$; *lane 8*, 500 nM unlabeled CaM, extract, cross-linker, and $CaCl_2$; *lane 9*, 0.1 mM trifluoperazine, extract, cross-linker, and $CaCl_2$; *lane 10*, IOVs, cross-linker, and $CaCl_2$; and *lane 11*, IOVs and cross-linker without $CaCl_2$.

neurin by chemical cross-linking (14). ^{125}I-CaM and solubilized binding proteins were covalently cross-linked with Lomant's reagent (41) and studied with SDS-PAGE autoradiography (Fig. 13). ^{125}I-CaM migrated as a single band of M_r = 17,000 even after cross-linking in the presence or absence of Ca^{2+}. Two discrete bands were found when ^{125}I-CaM was cross-linked to solubilized binding proteins in the presence of Ca^{2+} (*lane 4*). A M_r = 40,000 protein was prominent (M_r ~ 57,000 when cross-linked to ^{125}I-CaM). There was also a smaller amount of M_r = 8,000 protein (M_r ~ 25,000 when cross-linked to ^{125}I-CaM). The binding was Ca^{2+}-dependent (*lanes 5* and *11*) and inhibited by trifluoperazine (*lane 9*). The interaction appeared saturable since 20–100 nM unlabeled CaM inhibited ^{125}I-CaM binding by 50% (*lanes 6–7*), so the M_r = 8,000 and 40,000 proteins may correspond to class *Y* sites (Fig. 12). Some radioactivity appeared on top of the lanes. This consisted of ^{125}I-CaM bound to spectrin dimer (M_r = 460,000) and large ^{125}I-CaM aggregates which were separated on more porous gels (not shown). The low affinity large capacity sites (class *Z*, Fig. 12) probably correspond to spec-

trin, since purified spectrin dimer will cross-link to ^{125}I-CaM in the presence of Ca^{2+} (not shown). Neither M_r = 8,000 nor 40,000 protein was found free in the cytosol (not shown). Little M_r = 40,000 protein remained on IOVs while about half of the M_r = 8,000 band remained (Fig. 13, *lane 10*). If estimates of K_D from Fig. 12 apply to IOVs, it is likely that these contribute to the lower affinity sites (Fig. 8*C*). It is unlikely that the M_r = 8,000 and 40,000 proteins are degradation products of the Ca^{2+} transporter since they appear without variation under a variety of extraction conditions, and there is no evidence of proteolytic degradation of ankyrin (42) or protein 4.1 (not shown). Also, there are too many copies of these proteins for them to be derived from the Ca^{2+} transporter, and their appearance is not accompanied by activation of (Ca^{2+} + Mg^{2+})-ATPase. Cross-linking of ^{125}I-CaM to the M_r ~ 150,000 Ca^{2+} transporter was inefficient under these conditions but has been accomplished with a photoaffinity label (34). Altogether these observations are most consistent, with the high affinity sites on IOVs corresponding to the Ca^{2+} transporter and the M_r = 8,000 and 40,000 proteins representing a new class of CaM-binding proteins.

DISCUSSION

This report describes detailed studies of binding of ^{125}I-CaM to sites in human erythrocyte membranes which include the Ca^{2+} transporter as well as two new CaM-binding proteins. The two high affinity CaM-binding proteins of M_r = 8,000 and 40,000 are not likely to be structural proteins since they make up <8 pmol/mg of ghost protein (~1700 copies per cell). These proteins might be CaM-sensitive enzymes or regulatory subunits of enzymes, and it would not be surprising if the erythrocyte should have multiple CaM-dependent enzymes. Micromolar concentrations of CaM would be sufficient to drive several enzyme systems in addition to the Ca^{2+} transporter, and it is quite possible that other phenomena such as Ca^{2+}-induced K^+ efflux could be CaM mediated (43). Azido-^{125}I-CaM has been employed under conditions which optimized photoaffinity labeling of the Ca^{2+} transporter, yet much of the label was associated with other proteins in the IOVs including a band of M_r ~ 40,000 (34). The present study describes extraction and chemical cross-linking methods permitting more direct evaluation of two CaM-binding proteins of M_r = 8,000 and 40,000 with conditions producing only minimal cross-linking to the Ca^{2+} transporter of IOVs (Fig. 13).[2] Elucidation of the function of these two new proteins may provide insight into additional roles of CaM in the erythrocyte, and this is currently under investigation.

Membrane binding of ^{125}I-CaM was very slow at concentrations near 1 nM where binding to the Ca^{2+} transporter is predominant and required several hours to reach equilibrium (Fig. 7). CaM activation of (Ca^{2+} + Mg^{2+})-ATPase (44) and binding of ^{125}I-CaM to erythrocyte ghosts (21, 22) were both interpreted as positively cooperative interactions. Both phenomena might be explained by incomplete binding at the lowest CaM concentrations, for neither were observed in this study when sufficiently long incubations were employed. However, both were observed after short incubations (data not shown). CaM at 1 nM activated (Ca^{2+} + Mg^{2+})-ATPase after a lag period, but this was eliminated by preincubating membranes with CaM (45). The binding rate, as expected for a bimolecular reaction, was driven much faster at higher concentrations of CaM (Fig. 7). Experimental observations of high affinity interactions require unphysiologic dilutions of CaM (10^{-9} M), and nonequilibrium experiments are vulnerable to artifact resembling positive cooperativity due to the slow rate of binding. Also, extraction of native CaM from erythrocyte ghosts may be incomplete due to slow reversal of binding. It was found that the ghosts and IOVs used in this study retained <0.1% of basal erythrocyte CaM (Table I), while a 10- to 20-fold higher level of residual CaM was reported with high basal (Ca^{2+} + Mg^{2+})-ATPase activity (46).

Binding of ^{125}I-CaM to erythrocyte membranes increased as free Ca^{2+} rose from pCa^{2+} 8 to pCa^{2+} 6.4. Erythrocyte cytosolic free Ca^{2+} concentrations were thought to be ~10^{-6} M (9), but free Ca^{2+} is difficult to measure. Nondisruptive introduction of an intracellular chelator has shown the resting erythrocyte free Ca^{2+} to be approximately 2 × 10^{-8} M (47). Physiological shear stresses have been found to greatly enhance Ca^{2+} influx (48). Therefore, it is likely that the Ca^{2+} transporter must respond to a sudden influx of Ca^{2+} during turbulent arterial flow, pump out Ca^{2+} until the free concentration is 10^{-8} M, and then switch off. Ca^{2+} is considered an essential intracellular signal (49), and it is likely that the shear related influx of Ca^{2+} produces other CaM-mediated physiologic effects, perhaps a reversible contraction of the membrane skeleton mediated by the M_r = 8,000 or 40,000 CaM-binding proteins. A temporary contraction should help the cell survive rapid flow related stress and is probably distinct from the pathological Ca^{2+} effects produced by 10^{-3} M Ca^{2+} introduced with ionophores. The high affinity binding of CaM to membrane Ca^{2+} transporter would also be expected to rise dramatically as free Ca^{2+} rises above pCa^{2+} 8.0 (Fig. 3) and would fall off the membrane as the free Ca^{2+} is reduced (Fig. 6). The ATPase activity of the Ca^{2+} transporter, however, is negligible below pCa^{2+} 7.0 and rises to maximum activity near pCa^{2+} 5 (20). Thus there appears to be a discrepancy between the free Ca^{2+} range required for high affinity CaM binding (pCa^{2+} 8 − 6.4) and the concentration range required for activation of (Ca^{2+} + Mg^{2+})-ATPase (pCa^{2+} 7 − 5.5).

The discrepancy in Ca^{2+} requirements for membrane binding and (Ca^{2+} + Mg^{2+})-ATPase activation suggests that two steps are involved. CaM is known to have four different Ca^{2+} binding sites with micromolar affinities which fill in a preferred sequence, and probably all sites need not be filled in order for the complex to activate some enzymes (50). At submicromolar Ca^{2+} concentrations it is possible that CaM occupied by a single Ca^{2+} ion could bind to the (Ca^{2+} + Mg^{2+})-ATPase which could shift it to a potentially activated form, and a second step would be required for final activation. Perhaps CaM occupied by only one Ca^{2+} ion will bind to the enzyme but the CaM must be occupied by 2 or 3 additional Ca^{2+} ions in order for it to completely activate the enzyme. Alternatively, once CaM has bound to the regulator site on the enzyme, additional Ca^{2+} ions may activate the enzyme directly by binding to the catalytic site of the enzyme as substrate. This hypothesis is likely since partial proteolysis removes the CaM binding regulator site of the enzyme. The digested enzyme is no longer dependent upon CaM but is still dependent upon free Ca^{2+} very much like the CaM-activated enzyme (20, 36). The K_D of CaM for Ca^{2+} and the K_M of Ca^{2+} transporter for Ca^{2+} are both in the micromolar range which is consistent with the Ca^{2+} concentration being rate limiting for both steps.

Measurement of ^{125}I-CaM binding to erythrocyte ghosts and IOVs may be useful in evaluating clinical disorders such as Duchenne muscular dystrophy (51, 52) or sickle cell anemia

[2] Photoactivated affinity cross-linkers such as azido-CaM react quickly and randomly with a variety of carbon-hydrogen bonds, whereas the chemical cross-linker, Lomant's reagent, is longer lived and specifically reacts with nucleophiles such as amines. Therefore, studies performed by these different methods of cross-linking may not produce identical results.

(53), where abnormalities of $(Ca^{2+} + Mg^{2+})$-ATPase have been reported. This assay may also be useful in evaluation and development of specific antagonists of calmodulin action.

Acknowledgments—Instructive discussions with Drs. Velia Fowler and Kenneth M. M. Murphy are appreciated. We also thank Brian Halligan and George Turner, who assisted with portions of this project, Donna Gardner, who drew figures, Arlene Daniel, who typed the manuscript, and Dr. James Bartles for helpful criticism of the manuscript.

REFERENCES

1. Cheung, W. Y. (ed) (1980) *Calcium and Cell Function, Vol. 1, Calmodulin,* Adademic Press, New York
2. Cheung, W. Y. (1980) *Science* **207,** 19–27
3. Means, A. R., and Dedman, J. R. (1980) *Nature (Lond.)* **285,** 73–77
4. Klee, C. B., Crouch, T. H., and Richman, P. G. (1980) *Annu. Rev. Biochem.* **49,** 489–515
5. Gopinath, R. M., and Vincenzi, F. F. (1977) *Biochem. Biophys. Res. Commun.* **77,** 1203–1209
6. Jarrett, H. W., and Penniston, J. T. (1977) *Biochem. Biophys. Res. Commun.* **77,** 1210–1216
7. Jarrett, H. W., and Penniston, J. T. (1978) *J. Biol. Chem.* **253,** 4676–4682
8. Larsen, F. L., and Vincenzi, F. F. (1979) *Science* **204,** 306–309
9. Schatzman, H. J. (1975) *Curr. Top. Membr. Transp.* **6,** 125–168
10. Weed, R. I., LaCelle, P. L., and Merrill, E. W. (1969) *J. Clin. Invest.* **48,** 795–809
11. Vandermeers, A., Robberecht, P., Vandermeers-Piret, M.-C., Rathe, J., and Christophe, J. (1978) *Biochem. Biophys. Res. Commun.* **84,** 1076–1081
12. Goewert, R. R., Landt, M., and McDonald, J. M. (1982) *Biochemistry* **21,** 5310–5315
13. LaPorte, D. C., and Storm, D. R. (1978) J. Biol. Chem. **253,** 3374–3377
14. Richman, P. G., and Klee, C. B. (1978) *J. Biol. Chem.* **253,** 6323–6326
15. Carlin, R. K., Grab, D. J., and Siekevitz, P. (1981) *J. Cell Biol.* **89,** 449–455
16. Sobue, K., Muramoto, Y., Fujita, M., and Kakiuchi, S. (1981) *Biochem. Biophys. Res. Commun.* **100,** 1063–1070
17. Glenney, J. R., Jr., Glenney, P., Osborn, M., and Weber, K. (1982) *Cell* **28,** 843–854
18. Palfrey, H. C., Schiebler, W., and Greengard, P. (1982) *Proc. Natl. Acad. Sci. U. S.A.* **79,** 3780–3784
19. Niggli, V., Penniston, J. T., and Carafoli, E. (1979) *J. Biol. Chem.* **254,** 9955–9958
20. Niggli, V., Adunyah, E. S., and Carafoli, E. (1981) *J. Biol. Chem.* **256,** 8588–8592
21. Niggli, V., Ronner, P., Carafoli, E., and Penniston, J. T. (1979) *Arch. Biochem. Biophys.* **198,** 124–130
22. Graf, E., Filoteo, A. G., and Penniston, J. T. (1980) *Arch. Biochem. Biophys.* **203,** 719–726
23. Penniston, J. T., Graf, E., and Itano, T. (1980) *Ann. N. Y. Acad. Sci.* **356,** 245–257
24. Bennett, V., and Stenbuck, P. J. (1980) *J. Biol. Chem.* **255,** 2540–2548
25. Bolton, A. E., and Hunter, W. M. (1973) *Biochem. J.* **133,** 529–533
26. Bennett, V., and Branton, D. (1977) *J. Biol. Chem.* **252,** 2753–2763
27. Caldwell, P. C. (1970) in *Calcium and Cellular Functional* (Cuthbert, A. W., ed) pp. 10–16, Macmillan, London
28. Lowry, O. H., Rosebrough, N. J., Farr, A. L., and Randall, R. J. (1951) *J. Biol. Chem.* **193,** 265–275
29. Chafouleas, J. G., Dedman, J. R., Munjaal, R. P., and Means, A. R. (1979) *J. Biol. Chem.* **254,** 10262–10267
30. Weiss, B., Fertel, R., Figlin, R., and Uzunov, P. (1974) *Mol. Pharmacol.* **10,** 615–625
31. Rodbard, D., and Feldman, H. A. (1975) *Methods Enzymol.* **36,** 3–16
32. Drickamer, L. K. (1975) *J. Biol. Chem.* **250,** 1952–1954
33. Jarrett, H. W., and Kyte, J. (1979) *J. Biol. Chem.* **254,** 8237–8244
34. Hinds, T. R., and Andreasen, T. J. (1981) *J. Biol. Chem.* **256,** 7877–7882
35. Sarkadi, B., Enyedi, A., and Gardos, G. (1980) *Cell Calcium* **1,** 287–297
36. Stieger, J., and Schatzmann, H. J. (1981) *Cell Calcium* **2,** 601–616
37. Cheung, W. Y. (1971) *J. Biol. Chem.* **246,** 2859–2869
38. Cohen, P. (1973) *Eur. J. Biochem.* **34,** 1–14
39. Tanaka, T., Naka, M., and Hidaka, H. (1980) *Biochem. Biophys. Res. Commun.* **92,** 313–318
40. Hummel, J. P., and Dreyer, W. J. (1962) *Biochim. Biophys. Acta* **63,** 530–532
41. Lomant, A. J., and Fairbanks, G. (1976) *J. Mol. Biol.* **104,** 243–261
42. Bennett, V. (1978) *J. Biol. Chem.* **253,** 2292–2299
43. Caroni, P., and Carafoli, E. (1982) *Proc. Natl. Acad. Sci. U. S. A.* **79,** 5763–5767
44. Downes, P., and Michell, R. H. (1981) *Nature (Lond.)* **290,** 270–271
45. Vincenzi, F. F., Hinds, T. R., and Raess, B. U. (1980) *Ann. N. Y. Acad. Sci.* **356,** 232–244
46. Lynch, T. J., and Cheung, W. Y. (1979) *Arch. Biochem. Biophys.* **194,** 165–170
47. Lew, V. L., Tsien, R. Y., Miner, C., and Bookchin, R. M. (1982) *Nature (Lond.)* **298,** 478–481
48. Larsen, F. L., Katz, S., Roufogalis, B. D., and Brooks, D. E. (1981) *Nature (Lond.)* **294,** 667–668
49. Rasmussen, H. (1970) *Science* **170,** 404–412
50. Wallace, R. W., Tallant, E. A., Dockter, M. E., and Cheung, W. Y. (1982) *J. Biol. Chem.* **257,** 1845–1854
51. Hodson, A., and Pleasure, D. (1977) *J. Neurol. Sci.* **32,** 361–369
52. Luthra, M. G., Stern, L. G., and Kim, H. D. (1979) *Neurology* **29,** 835–841
53. Niggli, V., Adunyah, E. S., Cameron, B. F., Bababunmi, E. A., and Carafoli, E. (1982) *Cell Calcium* **3,** 131–151
54. Scatchard, G. (1949) *Ann. N. Y. Acad. Sci.* **51,** 660–672
55. Laemmli, U. K. (1970) *Nature (Lond.)* **227,** 680–685